The Attitude Control System Concept for the Joint Australian Engineering Micro-Satellite (JAESat)

Aaron Dando*
Advisor: Werner Enderle†
Cooperative Research Center for Satellite Systems
Queensland University of Technology
GPO Box 2434, Brisbane, QLD, Australia, 4001

JAESat is a joint micro-satellite project between Queensland University of Technology (QUT), Australian Space Research Institute (ASRI) and other national and international partners including the Australian Cooperative Research Centre for Satellite Systems (CRCSS), Kayser-Threde GmbH, Aerospace Concepts and Auspace who will contribute to this project. The JAESat micro-satellite project is an educational and GNSS technology demonstration mission. The main objectives of the JAESat mission are the design and development of a micro-satellite in order to educate and train students and also to generate a platform in space for technology demonstration and conduction of research on a low-cost basis. The main payload on-board JAESat will be a GPS receiver called SPARx (SPace Applications Receiver), developed by the Queensland University of Technology for attitude and orbit determination. In addition to the GPS based attitude sensor, a star sensor will be on-board JAESat for attitude determination. JAESat will be three-axis stabilized based on a zero-momentum approach using magnetic coil actuators. This paper will outline the Attitude Control System (ACS) concept for JAESat including: subsystem configuration and components, performance requirements, control mode definition, attitude dynamic modeling, control law development, and attitude determination concept. Performance of the JAESat ACS is predicted via simulations using a comprehensive ACS model developed in Matlab Simulink.

I. Introduction

The JAESat micro-satellite project is an educational and Global Navigation Satellite Systems (GNSS) technology demonstration mission, which will also generate data for scientific use. The high level mission objectives[1,2] of JAESat are:

- Design, develop, manufacture, test, launch and operate the educational/research micro-satellite JAESat
- Develop payloads with a technological and scientific relevance
- Use JAESat as a sensor in space and GNSS technology demonstrator mission

As can be seen from the high level mission objectives, the education and training aspects play an important role in the JAESat mission. The GNSS mission objective is driven by the SPARx (Space Applications GPS Receiver), a development by QUT/CRCSS. Functions and performance of SPARx will be tested and validated in space within the JAESat mission. Another key element of the high level mission objectives is the development and testing of a novel integrated attitude sensor concept combining star sensor and GPS attitude sensor data.

The JAESat mission will ultimately consist of two micro-satellites (master and slave) flying in formation (see Figure 1). The satellites will be coupled during the launch phase and then separated in space by a spring mechanism. Following the separation the two satellites will drift away from each other with a low drift rate (~ 0.01 m/s). A communication link between the two satellites will be established in form of a RF Inter-Satellite Link (ISL). The master satellite will be a cube with side length 390 mm and approximate mass 25 kg. The slave satellite will be half the height of the master satellite with dimensions 390 mm x 390 mm x 195 mm and approximate mass 15 kg.

Negotiations with prospective launch providers for a piggyback launch are ongoing and consequently the final orbit of JAESat has not yet been established. However, it is intended that JAESat will be placed into a circular, near-polar sun-synchronous Low Earth Orbit (LEO) with an orbit altitude between 600 km and 800 km. The operational life time of JAESat is expected to be approximately 12 months. Mission operations will be conducted from a ground station located at the Queensland University of Technology in Brisbane, Australia. JAESat will be designed to possess a high degree of on-board autonomy and to conduct a variety of experiments based on the mode of interoperation between the payloads on-board the two satellites.

* PhD Candidate, CRCSS at the Queensland University of Technology. Member IEEE. a.dando@qut.edu.au.
† Associate Professor, CRCSS at the Queensland University of Technology. Member IEEE. w.enderle@qut.edu.au.

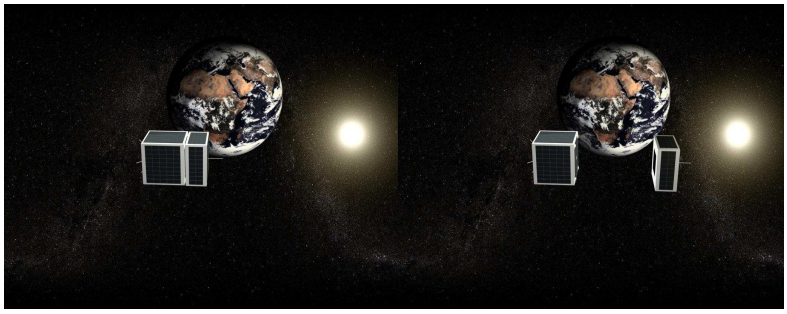

Figure 1: Separation of master satellite (left) and slave satellite (right) in space

The main experiments[3,4] for JAESat include:

- Testing and evaluation of the QUT/CRCSS SPARx, including attitude capability
- Testing of a new integrated star sensor/GPS sensor concept for three-axis attitude determination
- Relative navigation between JAESat master and slave satellites
- Orbit determination concepts:
  - On-ground precise orbit determination based on GPS code and carrier phase measurements
  - On-board orbit determination based on GPS receiver position solutions
- Relative positioning between master and slave satellites
- Establishment of stable RF inter-satellite link
- Atmospheric research

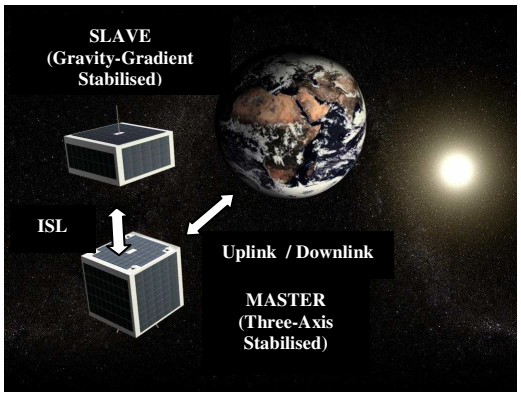

Figure 2: Inter-satellite and ground station communications concept for the JAESat mission

II. ACS Requirements

A preliminary set of ACS performance requirements has been derived for the Normal Mode of operations (see Table 1), driven primarily by the mission requirement to establish an ISL. The Detumbling Mode requirement is for the coupled satellite angular velocity to be damped to less than 0.2 deg/sec (per axis). During the Reorientation Mode in which the master and slave are still coupled, the requirements for the master satellite specified in Table 1 may be used. The orbit-average power consumption requirement for the master ACS in each operational mode is TBD.

	Accuracy	*Jitter*	*Settling Time*
MASTER	5 deg (per axis)	TBD	6 orbits (per axis)
SLAVE	10 deg (roll, pitch) 15 deg (yaw)	TBD	N/A

Table 1: Minimum pointing requirements (3σ) with baseline ACS components

III. Attitude Control System Concept

The key driver for the Attitude Control System (ACS) concept is the establishment of an ISL so that housekeeping and scientific data can be transferred between the two satellites. Communication with the ground station (uplink satellite commands and downlink telemetry) will be via the master satellite only. The communications concept for the JAESat mission is illustrated in Figure 2. To meet the important ISL mission requirement an innovative ACS concept is proposed comprising a three-axis stabilized master satellite and gravity-gradient stabilized slave satellite in formation flight. This concept aims to reduce the cost and complexity of future formation flying missions. In addition, system modularity will be a key feature of the low-cost master ACS design to accommodate modifications and improvements for different micro-satellite missions conducted in LEO.

Master Satellite

The master satellite will be three-axis stabilized using a zero-momentum approach. The baseline ACS will provide three-axis attitude determination and control for large-angle tracking/slewing maneuvers and also for fine pointing. A block diagram of the master ACS is depicted in Figure 3. Component selection was based on total system cost, requirements (functional and performance), availability, and system compatibility.

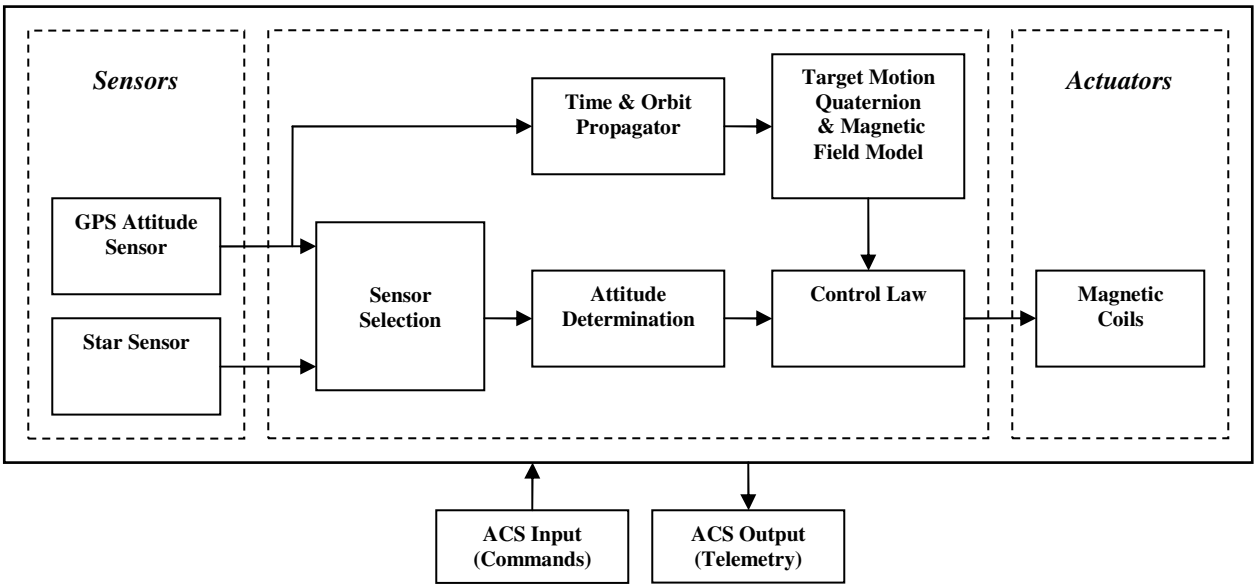

Figure 3: ACS block diagram for the JAESat master satellite

The actuator complement consists of three magnetic coil actuators with air cores (air coils) whose magnetic moment vectors are aligned with the satellite body axes. Three additional coils may be implemented to provide a certain level of redundancy in the ACS design. The air coils are to be designed and manufactured at QUT. Preliminary design parameters for the air coils using SWG-18 copper wire are summarized in Table 2.

MASS	0.57 kg
COIL AREA	0.15 m^2
NO. OF TURNS	50
RESISTIVITY OF COPPER WIRE	$1.7e^{-8}$ Ωm
WIRE CROSS-SECTIONAL AREA	$0.823e^{-6}$ m^2
COIL RESISTANCE	1.6 Ω
SATURATION MOMENT	10 Am^2
MAX. COIL CURRENT	1.3 A
MAX. POWER CONSUMPTION AT SATURATION (COIL ONLY)	2.8 W

Table 2: Preliminary design parameters for a single air coil

The baseline sensor complement consists of an integrated attitude sensor comprising a star sensor and multi-antenna GPS sensor. This concept has been previously investigated[5-7] by the German Space Operations Center (GSOC) for three-axis attitude determination. It aims to overcome many of the performance and functional limitations of conventional attitude sensors whilst also providing critical navigation data and precise timing. The boresight axis of the star sensor will be aligned with the +z body axis. The four GPS antennas will be located at the corners of the +z face of the master (see Figure 10), thus providing an unobstructed half sphere field-of-view. The ground link and inter-satellite link antennas will be located on the –z and +x faces respectively. During the Normal Mode the +z body axis will point in the zenith direction allowing for the best possible visibility of the GPS satellite constellation and reference stars so that a continuous attitude solution will be available.

A KM-1303 star sensor[8] has been contributed by Kayser-Threde GmbH for use in the JAESat project (see Table 3). The major operational limitation of star sensors is their sensitivity to large rotation rates (> 5 deg/sec) leading to star identification difficulties and consequently an erroneous attitude solution. However, by using additional external information from the GPS attitude sensor, the probability of correctly identifying star patterns will improve substantially.

DIMENSIONS	Star sensor body: 112 × 115 × 45 mm Height: 170 mm (with baffle)
MASS	Sensor unit: 0.58 kg 16 mm lens: 0.1 kg Baffle: ca. 0.1 kg
POWER	Power consumption max.: 5 W Power consumption typical at 12 VDC: 4.2 W Input voltage range: 12 - 15 VDC Connector type: DSUB 9 pin
STAR SENSOR PERFORMANCE	Field of view: 21° × 31° Sensitivity: MV = +6 to -2 Update period: 250 ms Star acquisition time: 0.5 s (first acquisition) Accuracy: ± 0.02° (2 Sigma)

Table 3: Key characteristics and specifications of the Kayser-Threde KM-1301 star sensor

The GPS based three-axis attitude sensor will be designed and manufactured at QUT. It will use the low-cost, lightweight SPARx technology which is based on the MITEL GP2021, GP2015, and GP2010 chip set and is a modification of the MITEL Orion[9] GPS receiver demonstrator. Each GPS SPARx unit is 95 mm x 50 mm x 50 mm with 12 parallel channels and has a power consumption of approximately 2W (including active antenna).

All ACS processing for the master will be performed by the on-board flight computer, a low-cost commercial-off-the-shelf Intrinsyc® Cerf™ Board. Specific features include a 192 MHz Intel™ Strongarm™ CPU, 16 MB flash memory, 32 MB SDRAM, and three RS232 serial ports.

Slave Satellite

The slave satellite will be gravity-gradient stabilised without using a deployable boom or libration damper. Hence the satellite inertia matrix will need to be designed to ensure gravity-gradient stabilization within the requirements specified in Table 1.

IV. ACS Operational Modes

***Detumbling Mode*:** This mode will use a simple B-dot control law to damp the angular rates of the coupled satellite (master and slave) relative to the earth's magnetic field.

***Reorientation Mode*:** This mode will use a star sensor based inertial attitude solution and a tracking maneuver control law to reorientate the coupled satellite so that it tracks reference frame 1 (defined in Table 4), within the accuracy specified in Table 1. Once the tracking maneuver has been completed the slave satellite will be correctly orientated for gravity-gradient stabilisation and the two satellites will then be separated.

ORIGIN	Master satellite mass center
X-AXIS	Toward the center of the earth or nadir ($-\hat{\mathbf{r}}$)
Y-AXIS	Direction of specific angular momentum vector or orbit plane normal ($\hat{\mathbf{r}} \times \hat{\mathbf{v}}$)
Z-AXIS	Completes right-hand orthogonal set

Table 4: Definition of reference frame 1

***Normal Mode*:** This is the primary mode for the JAESat mission during which a number of experiments will be conducted (see section I). Following the separation an ISL will be established between the two satellites. In this mode the slave will be gravity-gradient stabilised and the master will be three-axis stabilised tracking reference frame 2 (defined in Table 5), within the accuracy specified in Table 1. The master will use the same control and attitude determination algorithms as the Reorientation Mode. Also during this mode the master will test and validate the novel attitude sensor concept for three-axis attitude determination.

ORIGIN	Master satellite mass center
X-AXIS	Completes right-hand orthogonal set
Y-AXIS	Direction of the specific angular momentum vector or orbit plane normal ($\hat{\mathbf{r}} \times \hat{\mathbf{v}}$)
Z-AXIS	Direction of satellite position vector or zenith ($\hat{\mathbf{r}}$)

Table 5: Definition of reference frame 2

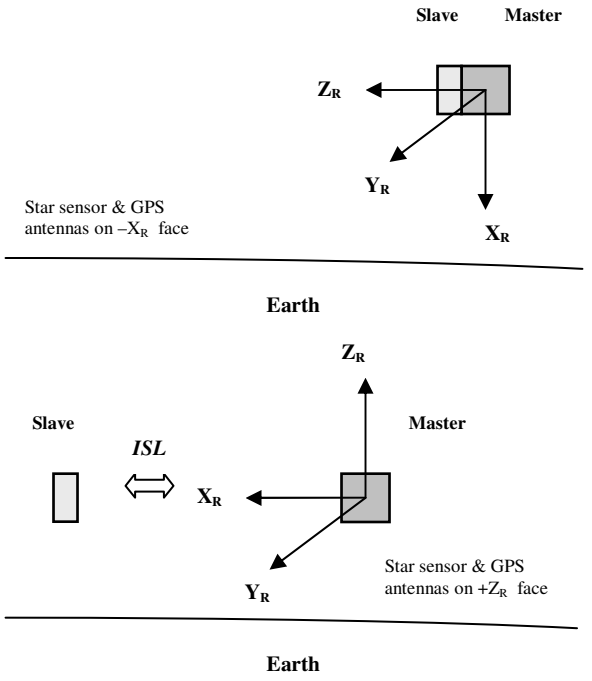

Figure 4: Reorientation and Normal ACS operational modes

V. Attitude Modeling

This section will present (without derivation) the dynamic and kinematic equations of motion for the three-axis stabilised JAESat master satellite. Both attitude regulation and attitude tracking will be considered. All vectors are expressed in the master satellite body frame (origin at satellite mass center).

Kinematic Equations of Motion

For *attitude regulation* the objective is to stabilise the satellite body frame with respect to an inertial (non-rotating) reference frame. For this case the kinematic equations of motion are given by:

$$\dot{\mathbf{q}} = \frac{1}{2}\boldsymbol{\Xi}(\mathbf{q})\boldsymbol{\omega} \tag{1}$$

$$\boldsymbol{\Xi}(\mathbf{q}) = \begin{bmatrix} [\mathbf{q}_{13}\times] + q_4\mathbf{I}_{3\times 3} \\ -\mathbf{q}_{13}^{\mathrm{T}} \end{bmatrix} \tag{2}$$

where $\boldsymbol{\omega}$ is the angular velocity of the body frame relative to the inertial frame, $\mathbf{I}_{nxn}$ is an n x n identity matrix, $[\cdot\times]$ denotes the vector cross product operator, and $\mathbf{q}$ is a quaternion describing the orientation of the body frame relative to the inertial frame. The attitude quaternion is defined as:

$$\mathbf{q} = \begin{bmatrix} \mathbf{q}_{13} \\ q_4 \end{bmatrix} \tag{3}$$

$$\mathbf{q}_{13} = \begin{bmatrix} q_1 \\ q_2 \\ q_3 \end{bmatrix} = \hat{\mathbf{n}} \sin\left(\frac{\Phi}{2}\right) \tag{4a}$$

$$q_4 = \cos\left(\frac{\Phi}{2}\right) \tag{4b}$$

where $\hat{\mathbf{n}}$ is a unit vector in the direction of Euler axis of rotation and Φ is the angle of rotation. Since the quaternion is a non-minimal parameterisation of the attitude an additional parameter is required which is related through the constraint equation:

$$\mathbf{q}^T\mathbf{q} = \mathbf{q}_{13}^T\mathbf{q}_{13} + q_4^2 = 1 \tag{5}$$

For *attitude tracking* the objective is to stabilise the satellite body frame with respect to a rotating reference frame defined in terms of a desired quaternion $\mathbf{q}_d$ and angular velocity $\boldsymbol{\omega}_d$. The error quaternion describing the orientation of the body frame relative to the rotating reference frame is defined as:

$$\delta\mathbf{q} = \mathbf{q} \otimes \mathbf{q}_d^{-1} \tag{6}$$

where the $\otimes$ operator denotes quaternion multiplication[10]. This may also be expressed as:

$$\delta\mathbf{q} = \boldsymbol{\Psi}(\mathbf{q})\mathbf{q}_d \tag{7}$$

$$\boldsymbol{\psi}(\mathbf{q}) = \begin{bmatrix} -\boldsymbol{\Xi}^T(\mathbf{q}) \\ \mathbf{q}^T \end{bmatrix} \tag{8}$$

The error angular velocity describing the angular velocity of the body frame relative to the rotating reference frame is defined as:

$$\delta\boldsymbol{\omega} = \boldsymbol{\omega} - \boldsymbol{\omega}_d \tag{9}$$

Hence for attitude tracking the kinematic equations of motion are given by:

$$\delta\dot{\mathbf{q}} = \frac{1}{2}\boldsymbol{\Xi}(\delta\mathbf{q})\delta\boldsymbol{\omega} \tag{10}$$

Dynamic Equations of Motion

The (rigid body) dynamic equations of motion for the JAESat master satellite are given by:

$$\dot{\boldsymbol{\omega}} = -\mathbf{J}^{-1}[\boldsymbol{\omega}\times]\mathbf{J}\boldsymbol{\omega} + \mathbf{J}^{-1}\mathbf{T}_{gg} + \mathbf{J}^{-1}\mathbf{T} \tag{11}$$

where $\boldsymbol{\omega}$ is the angular velocity of the body frame relative to the inertial frame, $\mathbf{J}$ is the satellite inertia matrix, $\mathbf{T}$ is the external control torque generated by the magnetic coils, and $\mathbf{T}_{gg}$ is the gravity-gradient disturbance torque. The control torque is defined by:

$$\mathbf{T} = [\mathbf{m}\times]\mathbf{B} \tag{12}$$

where $\mathbf{m}$ is the magnetic moment generated by the magnetic coils, and $\mathbf{B}$ is the magnetic flux density of the earth's magnetic field at the satellite location (also called geomagnetic field vector). The earth's main magnetic field is modeled using a 10th order IGRF model with extrapolated J2005 coefficients. Each magnetic coil produces a magnetic moment according to:

$$m = NAI \tag{13}$$

where N is the number of turns of wire, A is the area formed by the coil, and I is the coil current. The gravity-gradient torque is given by:

$$\mathbf{T}_{gg} = 3\omega_0^2[\hat{\mathbf{r}}\times]\mathbf{J}\hat{\mathbf{r}} \tag{14}$$

where $\hat{\mathbf{r}}$ is a unit vector in the zenith direction, and ω_0 is the orbit angular velocity. For the case of *attitude regulation* Eq (11) can be used directly. For *attitude tracking* the dynamic equations of motion are obtained by differentiating Eq (9) and substituting the result into Eq (11) which leads to the following expression:

$$\delta\dot{\boldsymbol{\omega}} = -\mathbf{J}^{-1}[\boldsymbol{\omega}\times]\mathbf{J}\boldsymbol{\omega} - \dot{\boldsymbol{\omega}}_d + \mathbf{J}^{-1}\mathbf{T}_{gg} + \mathbf{J}^{-1}\mathbf{T} \tag{15}$$

VI. Attitude Control Laws

This section presents the control laws that will be implemented in the master ACS during each mode of operation. For each control law (including derivations) all vectors are expressed in the master satellite body frame unless otherwise specified. Performance of the closed-loop system is simulated using a comprehensive ACS model developed in Matlab® Simulink. For all simulations perfect attitude knowledge has been assumed, i.e. attitude determination using ideal sensors

```
FEDSAT
1 27598U 02056B   05122.26089911 -.00000001  00000-0  17045-4 0  6439
2 27598  98.5672 196.2324 0009070 346.7664  13.3272 14.27886601124186
```

Table 6: Two-Line Element Set for FedSat

with zero noise, infinite bandwidth, and zero misalignment. The satellite orbit state vector information is based on the SGP4 algorithm using NORAD Two-Line Elements (TLE) for the 800km sun-synchronous orbit of FedSat (see Table 6).

Detumbling Mode

Three-axis magnetic moment commands for the magnetic coils are generated using a simple B-dot control law[11]:

$$\mathbf{m} = -\mathbf{K}\dot{\mathbf{B}} \tag{16}$$

where $\mathbf{K}$ is a positive definite diagonal gain matrix and $\dot{\mathbf{B}}$ is the time derivative of the body frame components of the geomagnetic field vector.

Parameter	*Value*	*Units*
Inertia Matrix	$\mathbf{J} = \begin{bmatrix} 1.8 & 0 & 0 \\ 0 & 2.0 & 0 \\ 0 & 0 & 1.0 \end{bmatrix}$	kgm^2
Initial Attitude (1-2-3 Euler Angles)	$(\phi_0, \theta_0, \psi_0) = [0.0 \quad 0.0 \quad 0.0]^T$	rad
Initial Angular Rates	$\delta\omega_0 = [0.052 \quad 0.052 \quad 0.052]^T$	rad/sec
Gain Matrix	$\mathbf{K} = \begin{bmatrix} 2.5e^6 & 0 & 0 \\ 0 & 2.5e^6 & 0 \\ 0 & 0 & 2.5e^6 \end{bmatrix}$	Am^2s/T
Simulation Duration	18000	sec

Table 7: Parameters for Detumbling Mode simulation

Figure 5 shows that the coupled satellite angular velocities are damped to less than 0.2 deg/sec (with respect to reference frame 1) in approximately one orbit, which is compliant with the requirements specified in section II. The values in Table 7 were selected by trading-off system settling time for magnetic coil power consumption.

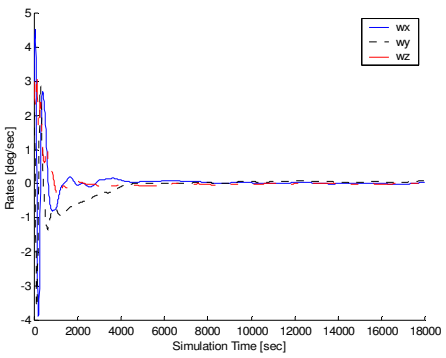

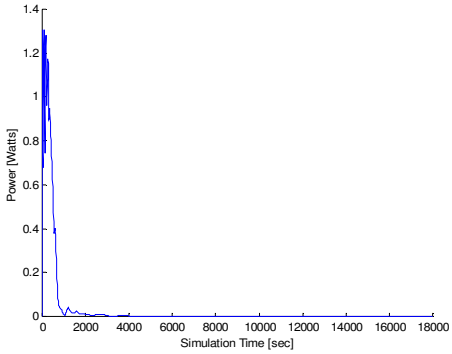

Figure 5: Satellite angular rates and total magnetic coil power consumption during Detumbling Mode

Reorientation Mode

Significant research efforts have been made to develop closed-loop control laws for large-angle attitude tracking maneuvers.[12-18] The control law to be implemented in the JAESat master satellite was developed by Crassidis, Vadali, and Markley for the NASA Microwave Anisotropy Probe (MAP) mission.[17,18] It is based on a variable-structure (sliding mode) control approach with optimal switching surfaces and is an extension of previous research conducted by Vadali on large-angle slew maneuvers.[19] The principle advantage of sliding mode control is its robustness with respect to satellite modeling uncertainties and unexpected disturbance torques.

To obtain the optimal switching surfaces a control law of the form $\boldsymbol{\omega} = \boldsymbol{\omega}(\mathbf{q})$ is sought which minimizes the following performance index:

$$\Pi = \lim_{t\to\infty}\left[\frac{1}{2}\int_{t_s}^{t}\left(\rho\delta\mathbf{q}_{13}^T\delta\mathbf{q}_{13}+\delta\boldsymbol{\omega}^T\delta\boldsymbol{\omega}\right)dt\right] \tag{17}$$

subject to Eq (1), where ρ is a scalar gain and t_s is the time of arrival at the sliding manifold. The Hamiltonian associated with minimising Eq (17) is defined as:

$$H = \frac{1}{2}\rho\delta\mathbf{q}_{13}^T\delta\mathbf{q}_{13} + \frac{1}{2}\delta\boldsymbol{\omega}^T\delta\boldsymbol{\omega} + \boldsymbol{\lambda}^T\dot{\mathbf{q}} \tag{18}$$

where $\boldsymbol{\lambda}$ is the costate vector associated with $\mathbf{q}$.

The necessary conditions for optimality according to Pontryagin's Minimum Principle are:

$$\dot{\mathbf{q}} = \frac{\partial H}{\partial \lambda} \tag{19a}$$

$$\dot{\lambda} = -\frac{\partial H}{\partial \mathbf{q}} \tag{19b}$$

$$\mathbf{0} = \frac{\partial H}{\partial \boldsymbol{\omega}} \tag{19c}$$

Using Eqs (1), (7), (8), (9), and (18) the solution of Eqs (19a)-(19c) leads to the following two-point boundary-value problem:

$$\dot{\mathbf{q}} = \frac{1}{2}\boldsymbol{\Xi}(\mathbf{q})\boldsymbol{\omega} \tag{20a}$$

$$\dot{\lambda} = -\rho\boldsymbol{\Xi}(\mathbf{q}_d)\boldsymbol{\Xi}^T(\mathbf{q}_d)\mathbf{q} + \frac{1}{2}\boldsymbol{\Xi}(\lambda)\boldsymbol{\omega} \tag{20b}$$

$$\boldsymbol{\omega} = -\frac{1}{2}\boldsymbol{\Xi}^T(\mathbf{q})\lambda + \boldsymbol{\omega}_d \tag{20c}$$

It can be shown based on analysis that the following choice for the sliding manifold minimizes Eqs (17) and (18):

$$\mathbf{s} = \boldsymbol{\delta\omega} + k\boldsymbol{\delta q}_{13} = \mathbf{0} \tag{21}$$

provided that $k = \pm\sqrt{\rho}$ where k is a scalar gain. It is critical to note that for the quaternion parameterisation of the attitude $\boldsymbol{\delta q}$ and $-\boldsymbol{\delta q}$ represent the same orientation, although the former gives the shortest distance to the sliding manifold whilst the later gives the longest distance. The sliding manifold defined by Eq (21) must therefore be modified to ensure that the attitude tracking maneuver follows the shortest possible path to the sliding manifold (and also to the reference trajectory):

$$\mathbf{s} = \boldsymbol{\delta\omega} + k\,\mathrm{sgn}\left[\delta q_4(t_s)\right]\boldsymbol{\delta q}_{13} = \mathbf{0} \tag{22}$$

It can be shown based on analysis and simulation that $\mathrm{sgn}[\delta q_4(t_s)]$ may be replaced with $\mathrm{sgn}[\delta q_4(t)]$ (denoted herein by $\mathrm{sgn}[\delta q_4]$) which also produces a maneuver to the reference trajectory in the shortest possible distance. Substituting Eq (22) into the derivative of Eq (7) leads to the following kinematic equations for "ideal sliding" on the sliding manifold:

$$\boldsymbol{\delta\dot{q}}_{13} = -\frac{1}{2}k\left|\delta q_4\right|\boldsymbol{\delta q}_{13} + \frac{1}{2}\left[\boldsymbol{\delta q}_{13}\times\right]\left(2\boldsymbol{\omega}_d - k\,\mathrm{sgn}\left[\delta q_4\right]\boldsymbol{\delta q}_{13}\right) \tag{23a}$$

$$\delta\dot{q}_4 = \frac{1}{2}k\,\mathrm{sgn}\left[\delta q_4\right]\left(1-\delta q_4^2\right) \tag{23b}$$

The trajectory in the state-space that slides on the sliding manifold can be shown to be asymptotically stable using Lyapunov's Direct Method. The following candidate Lyapunov function is proposed:

$$V = \frac{1}{2}\boldsymbol{\delta q}_{13}^T\boldsymbol{\delta q}_{13} \tag{24}$$

Substituting Eq (23a) into the derivative of Eq (24) leads to the following expression:

$$\dot{V} = -\frac{1}{2}k\left|\delta q_4\right|\boldsymbol{\delta q}_{13}^T\boldsymbol{\delta q}_{13} \tag{25}$$

which is clearly negative definite provided $k > 0$.

A control law is required so that the closed-loop system can asymptotically track a desired quaternion $\mathbf{q}_d$ and angular velocity $\boldsymbol{\omega}_d$. The equivalent control method[19,20] is used to develop a control law that induces ideal sliding based on external control torque inputs. It will be subsequently proven using a Lyapunov stability analysis that the same control law can also be used to force the state trajectory onto the sliding manifold. The dynamic and kinematic equations of motion for the attitude tracking case, given by Eqs (10) and (15), can be expressed as a system of *n* equations, linear in the *m* controls:

$$\dot{\mathbf{x}} = \mathbf{f}(\mathbf{x}) + \mathbf{BT} \tag{26}$$

where

$$\mathbf{x} = \begin{bmatrix}\boldsymbol{\delta q}\\ \boldsymbol{\delta\omega}\end{bmatrix} \tag{27}$$

$$\mathbf{f}(\mathbf{x}) = \begin{bmatrix}\boldsymbol{\delta\dot{q}}\\ -\mathbf{J}^{-1}\left[\boldsymbol{\omega}\times\right]\mathbf{J}\boldsymbol{\omega} + \mathbf{J}^{-1}\mathbf{T}_{gg} - \dot{\boldsymbol{\omega}}_d\end{bmatrix} \tag{28}$$

$$\mathbf{B} = \begin{bmatrix}\mathbf{0}_{4x3}\\ \mathbf{J}^{-1}\end{bmatrix} \tag{29}$$

During ideal sliding on the sliding manifold defined by $\mathbf{s} = \mathbf{0}$, $\dot{\mathbf{s}}$ can be set to zero:

$$\dot{\mathbf{s}} = \mathbf{P}\dot{\mathbf{x}} = \mathbf{Pf}(\mathbf{x}) + \mathbf{PBT}_{eq} = \mathbf{0} \tag{30}$$

where $\mathbf{T}_{eq}$ is the equivalent control torque and $\mathbf{P}$ is a *m* x *n* Jacobian matrix defined by:

$$\mathbf{P} = \frac{\partial \mathbf{s}}{\partial \mathbf{x}} = \begin{bmatrix} \frac{\partial s_1}{\partial x_1} & \cdots & \frac{\partial s_1}{\partial x_7} \\ \vdots & \ddots & \vdots \\ \frac{\partial s_3}{\partial x_1} & \cdots & \frac{\partial s_3}{\partial x_7} \end{bmatrix} \tag{31}$$

Using the definition of the sliding vector in Eq (22), the Jacobian matrix defined by Eq (31) reduces to:

$$\mathbf{P} = \begin{bmatrix} k\,\mathrm{sgn}[\delta q_4]\mathbf{I}_{3\times 3} & \mathbf{0}_{3\times 1} & \mathbf{I}_{3\times 3} \end{bmatrix} \tag{32}$$

The equivalent control torque can be obtained by rearranging Eq (30):

$$\mathbf{T}_{eq} = [\mathbf{PB}]^{-1}\mathbf{Pf}(\mathbf{x}) \tag{33}$$

which has a solution provided that [**PB**] is non-singular. Substituting Eqs (28), (29), and (32) into Eq (33) provides an expression for the equivalent control torque:

$$\mathbf{T}_{eq} = [\boldsymbol{\omega}\times]\mathbf{J}\boldsymbol{\omega} - \mathbf{T}_{gg} + \mathbf{J}[\dot{\boldsymbol{\omega}}_d - k\,\mathrm{sgn}[\delta q_4]\boldsymbol{\delta}\dot{\mathbf{q}}_{13}] \tag{34}$$

where $\boldsymbol{\delta}\dot{\mathbf{q}}_{13}$ is given by Eq (23a). Under the influence of additional external disturbance torques, unmodeled dynamics, parameter uncertainties and parameter variations, the equivalent control torque given by Eq (34) will not be sufficient to exactly maintain the ideal sliding motion. Hence it is necessary to modify $\mathbf{T}_{eq}$ in order to account for these non-ideal effects so that the state trajectory will remain close to the sliding manifold. The modified control law is selected as:

$$\mathbf{T} = \mathbf{T}_{eq} - \mathbf{JG}\upsilon \tag{35}$$

or

$$\mathbf{T} = [\boldsymbol{\omega}\times]\mathbf{J}\boldsymbol{\omega} - \mathbf{T}_{gg} + \mathbf{J}[\dot{\boldsymbol{\omega}}_d - k\,\mathrm{sgn}[\delta q_4]\boldsymbol{\delta}\dot{\mathbf{q}}_{13} - \mathbf{G}\upsilon] \tag{36}$$

where **G** is a 3 x 3 positive definite diagonal matrix and υ is a saturation function defined by:

$$\upsilon_i = \begin{cases} +1 & \text{for} \quad s_i > \varepsilon \\ \dfrac{s_i}{\varepsilon} & \text{for} \quad |s_i| \le \varepsilon \\ -1 & \text{for} \quad s_i < -\varepsilon \end{cases} \qquad i = 1,2,3 \tag{37}$$

where ε is a small positive scalar. The saturation function is used to minimise chattering in the control torque. The asymptotic stability of the closed-loop system using the control law given by Equation (36) can be assessed using Lyapunov's Direct Method. The following candidate Lyapunov function is proposed:

$$V = \frac{1}{2}\mathbf{s}^T\mathbf{s} \tag{38}$$

The derivative of the sliding vector in Eq (22) is obtained by assuming that $\mathrm{sgn}[\delta q_4]$ is constant with respect to time:

$$\dot{\mathbf{s}} = \boldsymbol{\delta}\dot{\boldsymbol{\omega}} + k\,\mathrm{sgn}[\delta q_4]\boldsymbol{\delta}\dot{\mathbf{q}}_{13} \tag{39}$$

The dynamic equations of motion for the attitude tracking maneuver are obtained by substituting Eq (36) into Eq (15):

$$\boldsymbol{\delta}\dot{\boldsymbol{\omega}} = -k\,\mathrm{sgn}[\delta q_4]\boldsymbol{\delta}\dot{\mathbf{q}}_{13} - \mathbf{G}\upsilon \tag{40}$$

Substituting Eqs (39) and (40) into the derivative of Eq (38) produces the following expression:

$$\dot{V} = -\frac{1}{2}\mathbf{s}^T\mathbf{G}\upsilon \tag{41}$$

which is negative definite provided that **G** is a positive definite matrix. Hence the control law given by Eq (36) may also be used to asymptotically force the state trajectory towards the sliding manifold.

As stated above, Eq (36) has been developed specifically for continuous external control torque inputs. The JAESat master satellite will use three orthogonal magnetic coils to generate the control torque. The fundamental limitation of using magnetic coils is that only the component of Eq (36) perpendicular to the geomagnetic field vector can be generated. This constraint follows directly from the definition of the magnetic torque given by Eq (12). The implication for closed-loop stability is that Lyapunov stability results given by Eqs (25) and (41) will not in general be valid for the magnetically actuated system. The following expression is used to generate the three-axis magnetic coil commands:

$$\mathbf{m} = \frac{\mathbf{B}\times\mathbf{T}^{\perp}}{\|\mathbf{B}\|^2} \tag{42}$$

where $\mathbf{T}^{\perp}$ is the component of Eq (36) perpendicular to the geomagnetic field vector. The control law parameters k, ε, and **G** must be carefully selected empirically so that the closed-loop system is asymptotically stable and the minimum performance requirements specified in Table 1 are achieved.

Parameter	*Value*	*Units*
Inertia Matrix	$\mathbf{J} = \begin{bmatrix} 1.8 & 0 & 0 \\ 0 & 2.0 & 0 \\ 0 & 0 & 1.0 \end{bmatrix}$	kgm^2
Initial Attitude (1-2-3 Euler Angles)	$(\phi_0, \theta_0, \psi_0) = \begin{bmatrix} \pi & 0 & \frac{\pi}{2} \end{bmatrix}^T$	rad
Initial Angular Rates	$\delta\omega_0 = [0.0035 \quad 0.0035 \quad 0.0035]^T$	rad/sec
Scalar Gain	$k = 0.001$	rad/sec
Deadband Constant	$\varepsilon = 0.01$	-
Saturation Gain Matrix	$\mathbf{G} = \begin{bmatrix} 2e^{-5} & 0 & 0 \\ 0 & 2e^{-5} & 0 \\ 0 & 0 & 2e^{-5} \end{bmatrix}$	/sec
Simulation Duration	40000	sec

Table 8: Parameters for Reorientation Mode simulation

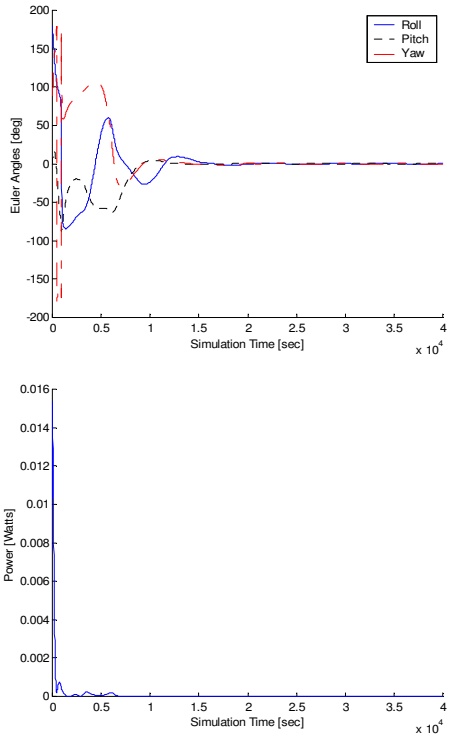

Figure 6: Satellite attitude and total magnetic coil power consumption during Reorientation Mode

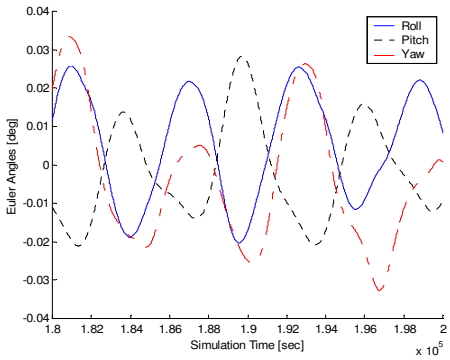

Figure 7: Steady-state pointing during Reorientation Mode

Figure 6 depicts the simulation of the large-angle tracking maneuver. The settling time for all axes is approximately the same and less than 30000 seconds. The steady-state pointing performance is depicted in Figure 7 and vastly exceeds the specified accuracy requirements. The magnetic coil power consumption is very low throughout the attitude tracking maneuver which is a key advantage of magnetic actuation.

Normal Mode

The control law defined by Eqs (36) and (42) can also be used for three-axis stabilisation of the master satellite during the Normal Mode.

Parameter	*Value*	*Units*
Inertia Matrix	$\mathbf{J} = \begin{bmatrix} 0.86 & 0 & 0 \\ 0 & 0.9 & 0 \\ 0 & 0 & 0.8 \end{bmatrix}$	kgm^2
Initial Attitude (1-2-3 Euler Angles)	$(\phi_0, \theta_0, \psi_0) = [0.35 \quad 0.35 \quad 0.35]^T$	rad
Initial Angular Rates	$\delta\omega_0 = 1e^{-5} * [1.75 \quad 1.75 \quad 1.75]^T$	rad/sec
Scalar Gain	$k = 0.001$	rad/sec
Deadband Constant	$\varepsilon = 0.01$	-
Saturation Gain Matrix	$\mathbf{G} = \begin{bmatrix} 4e^{-5} & 0 & 0 \\ 0 & 4e^{-5} & 0 \\ 0 & 0 & 4e^{-5} \end{bmatrix}$	/sec
Simulation Duration	40000	sec

Table 9: Parameters for Normal Mode simulation

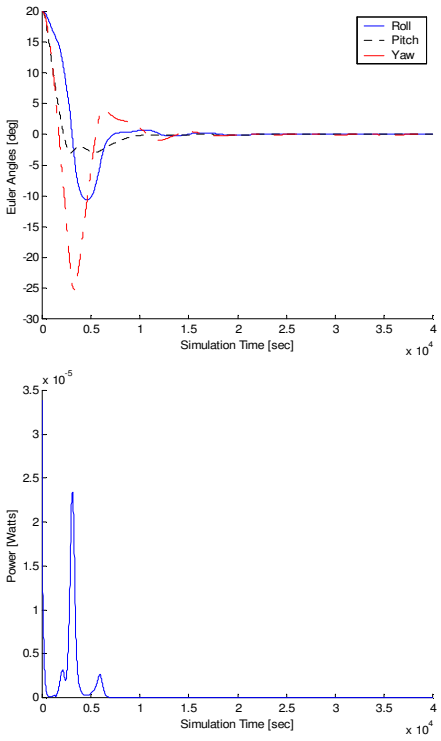

Figure 8: Satellite attitude and total magnetic coil power consumption during Normal Mode

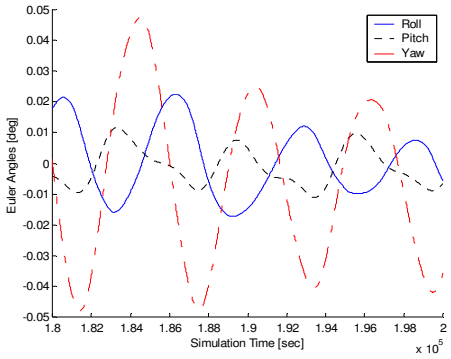

Figure 9: Steady-state pointing during Normal Mode

Results of the Normal Mode simulation provided in Figures 8 and 9 clearly show that the ACS is able to easily meet the performance requirements specified in Table 1. Alternative control strategies, for example proportional-derivative control or a Linear Quadratic Regulator (LQR) approach, will also be considered in future research in an attempt to improve the steady-state pointing performance with respect to Figure 9.

Simulations were also performed for both the Reorientation and Normal modes to investigate the robustness of the control law with respect to initial conditions and the satellite inertia matrix. Uncertainties of up to 15% in the moments of inertia and up to 25% in the rates were acceptable although the settling time was considerably degraded.

VII. Attitude Determination

Three-axis attitude determination (attitude and rates) for the master satellite will be performed by the star sensor and also by the attitude sensor based on GPS. However, the star sensor will be used predominately to provide attitude state information to the control algorithm. The GPS attitude sensor on the other hand will be used to test and validate different algorithms for GPS-based attitude determination and carrier phase cycle ambiguity resolution. It is also intended to conduct a series of tests where the benefits of this combination of attitude sensors will be clearly demonstrated. The star sensor directly outputs a quaternion estimate of the satellite three-axis attitude relative to an inertial reference frame (see Ref. 8 for further details). It also has the capability to provide star data information so that new algorithms can be tested for advanced star identification and attitude determination. Since rate gyros will not be included in the ACS design, the body rates will be derived from the star sensor output using the on-board flight computer. One possible method is to calculate the Euler axis/angle parameters for the angular motion between each sampling time step by differencing the current and previous quaternion estimates. The Euler angle is then divided by the sampling period and low-pass filtered to obtain the angular velocity about the Euler axis. Since the star sensor delivers directly an attitude solution, this section will concentrate on a brief description of the applied attitude determination concept based on GPS.

GPS Based Attitude Determination

The fundamental physical principle of the GPS based attitude determination process is the interferometric principle, which is depicted in Figure 10. The GPS receiver measures single (SD) or double (DD) carrier phase differences. As discussed in section 3, the master satellite will have four antennas arranged in a rectangular configuration on the +z satellite face (see Figure 10). It is intended that the master will use SD observations for the attitude determination process. The basic equations for the SD attitude determination algorithm[5,6] using Euler angles (rotation sequence 3-1-2) as attitude parameters will be presented below. The ideal observation equation (i.e. neglecting any error) is given by:

$$\Delta\Phi^{i}_{m} = \Delta\rho^{i}_{m} - \lambda\Delta N^{i}_{m} \qquad (43)$$

where $\Delta\Phi$ is the SD carrier phase, $\Delta\rho$ is the SD slant distance, λ is the wavelength of the GPS L1 signal, ΔN is the difference of the initial number of carrier phase cycle ambiguities, *m* is the index for the baseline, and *i* is the index for the GPS satellite pair that has been used to generate the SD observation. The SD slant distance as a function of the line-of-sight unit vector and the corresponding baseline vector is given by:

$$\Delta\rho^{i}_{m} = \left[\mathbf{A}(\phi,\theta,\psi)\mathbf{u}^{i}_{m}\right]\bullet\mathbf{b}_{m} \qquad (44)$$

where $\mathbf{A}(\phi,\theta,\psi)$ is the attitude matrix (reference frame to body frame), $\mathbf{u}$ is the line-of-sight unit vector expressed in the reference frame, and $\mathbf{b}$ is the baseline vector expressed in the body frame. Substituting Eq (44) into (43) and also considering an error term, leads to the general observation equation for SD carrier phase measurements:

$$\Delta\Phi^{i}_{m} = \left[\mathbf{A}(\phi,\theta,\psi)\mathbf{u}^{i}_{m}\right]\bullet\mathbf{b}_{m} - \lambda\Delta N^{i}_{m} + \Delta\varepsilon \qquad (45)$$

where $\Delta\varepsilon$ represents errors such as line bias, receiver noise and multipath effects. The carrier phase cycle ambiguity ΔN will be solved in an initialisation step for the attitude determination process with the STAR[7] algorithm based on spherical trigonometry. This method will also provide an initial guess for the state vector $\mathbf{x}$ defined as:

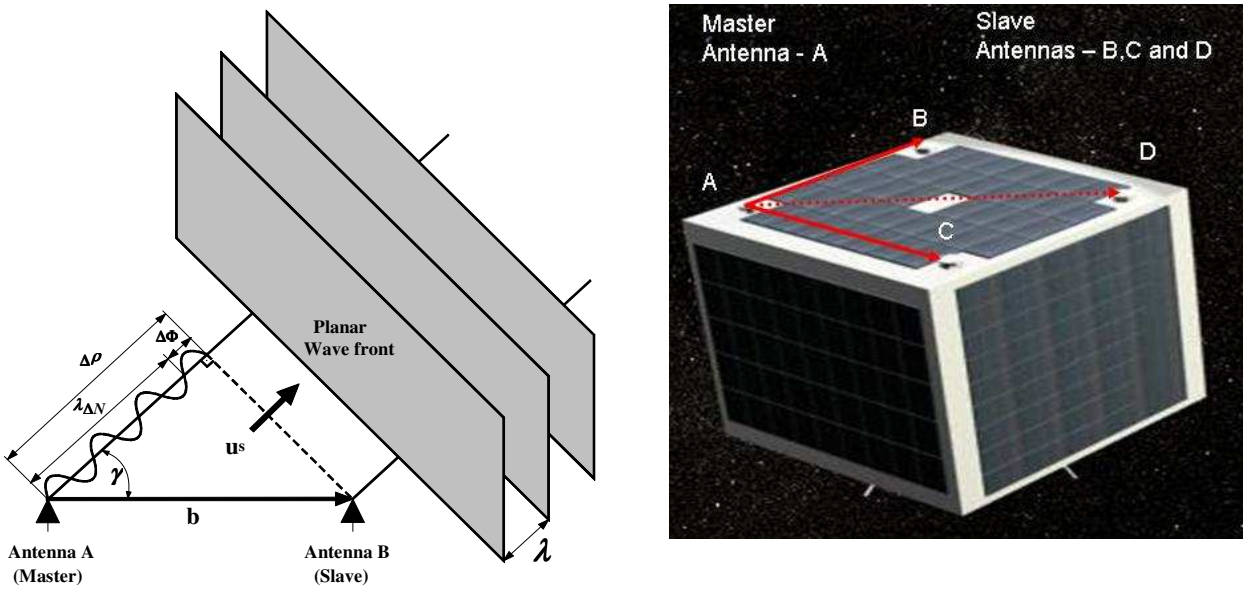

Figure 10: Interferometric principle and GPS attitude sensor array

$$\mathbf{x} = \begin{bmatrix} \phi & \theta & \psi \end{bmatrix}^T \tag{46}$$

A minimum of two visible GPS satellites are required in order to be able to perform a deterministic attitude solution. If more than two GPS satellites are visible, the number of measurements is larger than the number of unknown parameters, and therefore a Least Squares Solution (LSQ) will be used in a sequential way. The attitude determination solution will be obtained through the following expression:

$$\Delta\mathbf{x} = \left[\mathbf{M}^T\mathbf{M}\right]^{-1}\mathbf{M}^T\mathbf{l} \tag{47}$$

where $\Delta\mathbf{x} = [\Delta\phi\ \Delta\theta\ \Delta\psi]^T$ is the solution vector, $\mathbf{l}$ is a vector containing the residuals between calculated and measured observation, and $\mathbf{M}$ is a design matrix defined by:

$$\mathbf{M} = \left.\frac{\partial\Delta\Phi}{\partial\mathbf{x}}\right|_{\mathbf{x}=\mathbf{x}^*} \tag{48}$$

where $\mathbf{x}^*$ is the initial state vector. The LSQ attitude determination solution is given by:

$$\mathbf{x} = \mathbf{x}^* + \Delta\mathbf{x} \tag{49}$$

The accuracy of GPS based attitude determination is dependant upon the geometry, the baseline length and the measurement errors. It is commonly known that the most significant measurement error on the carrier phase results from multipath effects. The magnitude of the multipath strongly depends on the design of the satellite, in particular possible points and surfaces for the reflection of signals. Tests will be conducted to gain an understanding about the multipath effects for the JAESat master satellite. Currently a Gaussian distributed multipath error of 5mm (1σ, SD) has been assumed for simulation purposes. The one sigma attitude solution accuracy can be calculated using the following expressions:

$$\sigma_{\text{Yaw}} = \frac{\sigma_{\text{SD}}}{\text{b}}\,\text{YawDOP} \tag{50a}$$

$$\sigma_{\text{Roll}} = \frac{\sigma_{\text{SD}}}{\text{b}}\,\text{RollDOP} \tag{50b}$$

$$\sigma_{\text{Pitch}} = \frac{\sigma_{\text{SD}}}{\text{b}}\,\text{PitchDOP} \tag{50c}$$

$$\sigma_{\text{Att}} = \frac{\sigma_{\text{SD}}}{\text{b}}\,\text{AttDOP} \tag{50d}$$

where the attitude Dilution of Precision (DOP) is given by:

$$\text{ATTDOP} = \sqrt{\begin{matrix}\text{YawDOP}^2 + \text{PitchDOP}^2 \\ + \text{RollDOP}^2\end{matrix}} \tag{51}$$

The DOP values are obtained from the covariance matrix $\text{Cov} = [\mathbf{M}^T\mathbf{M}]^{-1}$ of the attitude solution.

VIII. Conclusion

In summary, an innovative low-cost ACS concept has been proposed for the JAESat mission. The proposed control law based on a sliding mode approach provides optimal large-angle slewing/tracking maneuvers and sub-degree steady-state pointing capabilities. The attitude determination concept is primarily based on the star sensor, but a novel integrated three-axis attitude sensor concept can be applied as well. The system performance of the JAESat master ACS has been verified through simulations and exceeds the specified minimum performance requirements, although the effect of using practical attitude sensors needs to be assessed. Further research and development will include implementation of the ACS software in the on-board flight computer and development of the integrated attitude sensor.

IX. Acknowledgements

The JAESat ACS R&D activities are being conducted at the Cooperative Research Centre for Satellite Systems, Queensland University of Technology. Special thanks to the CRCSS and all external project partners for their valuable contributions to the JAESat project.

Finally, I would like to thank Werner Enderle of QUT for reviewing the paper and providing critical feedback.

X. References

[1] Enderle, W. (2003). JAESat Project Documentation JAESat-GPS-PO-0001. *QUT Project Documentation*, Brisbane, Australia.

[2] Enderle, W. (2004). JAESat Mission Concept Description. *QUT Project Documentation*, Brisbane, Australia.

[3] Enderle, W., C. Boyd, and J.A. King. (2004). Joint Australian Engineering (Micro) Satellite (JAESat) - A GNSS technology demonstration mission. *Proceedings of the Global Navigation Satellite Systems*, Sydney, Australia.

[4] Enderle, W., A. Dando, and T. Bruggemann. (2005). The orbit and attitude determination concept for the Joint Australian Engineering (Micro) Satellite - JAESat. *Proceedings of the 28th Annual AAS Guidance and Control Conference*, Breckenridge, Colorado, USA.

[5] Arbinger, C., and W. Enderle. (2000). Spacecraft attitude determination using a combination of GPS attitude sensor and star sensor measurements. *Proceedings of the ION GPS Conference*, 2634-2642, Salt Lake City, Utah, USA.

[6] Arbinger, C., W. Enderle, and O. Wagner. (2001). GPS based star sensor aiding for attitude determination in high dynamics. *Proceedings of the ION GPS Conference*, 2952-2959, Salt Lake City, Utah, USA.

[7] Arbinger, C., W. Enderle, L. Fraiture, and O. Wagner. (1999). A new algorithm (STAR) for cycle ambiguity resolution within GPS based attitude determination. *Proceedings of the 4th ESA International Conference on Guidance, Navigation, and Control Systems*, 345-347, Noordwijk, The Netherlands.

[8] Kayser-Threde GmbH. (1998). KM-1301 Star Sensor User Manual.

[9] MITEL Semiconductors. (2001). GPS Orion 12 Channel GPS Reference Design AN4808.

[10] Shuster, M.D. (1993). A survey of attitude representations. *The Journal of the Astronautical Sciences*, 41(4): 439-517.

[11] Stickler, A.C., and K.T. Alfriend (1976). Elementary magnetic attitude control system. *Journal of Spacecraft and Rockets*, 13(5): 282-287.

[12] Vadali, S.R., and J.L. Junkins. (1984). Optimal open-loop and stable feedback control of rigid spacecraft attitude maneuvers. *The Journal of the Astronautical Sciences*, 32(2): 105-122.

[13] Wen, J. T-Y., and K. Kreutz-Delgado. (1991). The attitude control problem. *IEEE Transactions on Automatic Control*, 36(10): 1148-1162.

[14] Lo, S.C., and Y.P. Chen. (1995). Smooth sliding-mode control for spacecraft attitude tracking maneuvers. *Journal of Guidance, Control, and Dynamics*, 18(6): 1345-1349.

[15] Crassidis, J.L., and F.L. Markley. (1996). Sliding mode control using modified Rodrigues parameters. *Journal of Guidance, Control and* Dynamics, 19(6): 1381-1393.

[16] Robinett, R.D., and G.G. Parker. (1997). Least squares sliding mode control tracking of spacecraft large angle maneuvers. *The Journal of the Astronautical Sciences*, 45(4): 433-450.

[17] Crassidis, J.L., S.R. Vadali, and F.L. Markley. (1999). Optimal variable-structure control tracking of spacecraft maneuvers. *Proceedings of the NASA Flight Mechanics/Estimation Theory Symposium*, 201-214, Greenbelt, Maryland, USA.

[18] Crassidis, J.L., S.R. Vadali, and F.L. Markley. (2000). Optimal variable-structure control tracking of spacecraft maneuvers. *Journal of Guidance, Control, and Dynamics*, 23(3): 564-566.

[19] Vadali, S.R. (1986). Variable-structure control of spacecraft large angle maneuvers. *Journal of Guidance, Control, and Dynamics*, 9(2): 235-239.

[20] Utkin, V.I. (1977). Variable structure systems with sliding modes. *IEEE Transactions on Automatic Control*, 22(2): 212-222.

[21] Hughes, P.C. (1986). *Spacecraft Attitude Dynamics*. Canada: John Wiley and Sons.

[22] Wertz, J.R., ed. (2000). *Spacecraft Attitude Determination and Control*. Holland: Kluwer Academic Publishers.